3570 *Chem. Mater.* **2009,** *21,* 3570–3575
DOI:10.1021/cm901061c

CHEMISTRY OF MATERIALS
Article

Synthesis of Tributylphosphate Capped Luminescent Rare Earth Phosphate Nanocrystals in an Ionic Liquid Microemulsion

Chao Zhang,[†,‡] Ji Chen,*[,†] Xingfu Zhu,[§] Yunchun Zhou,[∥] and Deqian Li[†]

[†]*State Key Laboratory of Rare Earth Resource and Utilization, Changchun Institute of Applied Chemistry, Chinese Academy of Sciences, Changchun 130022, Jilin, China,* [‡]*Graduate School of the Chinese Academy of Sciences, Beijing 100049, China,* [§]*State Key Laboratory of Inorganic Synthesis and Preparative Chemistry, College of Chemistry, Jilin University, Changchun 130012, Jilin, China, and* [∥]*National Analytical Research Center of Electrochemistry and Spectroscopy, Changchun Institute of Applied Chemistry, Chinese Academy of Sciences, Changchun 130022, Jilin, China*

Received February 11, 2009

Uniform rare earth phosphate ($REPO_4$, RE = La−Tb) nanocrystals were successfully synthesized in a properly designed TBP/[Omim]Cl/H_2O (tributylphosphate/1-octyl-3-methyl-imidazolium chloride/water) microemulsion system. The phosphoryl groups anchored the TBP molecules on the surfaces of the nanocrystals, and this made the nanocrystals easily dispersed in some imidazolium-based ILs. $LaPO_4$:Eu^{3+} and $CePO_4$:Tb^{3+} nanocrystals capped with TBP showed bright red and green emission under UV excitation, with enhanced emission intensity and lifetimes compared with the uncapped ones. [Omim]Cl and TBP were found to play the key roles in the nucleation and growth of the nanocrystals. The designed strategy provided a facile way for the fabrication of TBP capped $REPO_4$ nanocrystals, which may also be applicable for the synthesis of other inorganic nanocrystals.

Introduction

Room temperature ionic liquids (RTILs) were generally defined as salts with low melting points, usually below 100 °C.[1] Many ionic liquids (ILs) were considered as "green" solvents with high thermal stability and nearly zero vapor pressures, thus widely used in synthetic chemistry, catalysis, separations, and electrochemistry,[1−7] and they were found to be very advantageous in the synthetic nanochemistry,[8−17] especially as templates[6,18] and capping agents.[19] In some "all in one" systems, ILs can actually play as solvent, template, and reagent.[12] Their particular phase behavior and unique physicochemical properties, including complexed solvation interactions with organic and inorganic compounds, can provide various growth pathways for nanocrystals with novel morphologies and properties,[20,21] such as the formation of rutile nanocrystals at a relatively low temperature,[9] high quality TiO_2 nanocrystals under microwave,[10] and highly conductive indium tin oxide nanocrystals.[14]

Microemulsions, isotropic liquid mixtures of oil, water, and surfactant, frequently in combination with a cosurfactant, were stable. In the binary systems (water/surfactant or oil/surfactant), diff erent types of self-assembled structures can be formed, providing excellent templating systems to synthesize monodispersed nanocrystals with controllable size and morphology.[22] Recently, imidazolium-based ILs had been explored and used as solvents of the inner phase, or continuous outer phase, or surfactants in the formation of microemusion systems.[23−27] Research

*To whom correspondence should be addressed. Tel/Fax: +86-431-85262646. E-mail: jchen@ciac.jl.cn.

(1) Welton, T. *Chem. Rev.* **1999**, *99*, 2071.
(2) Binnemans, K. *Chem. Rev.* **2007**, *107*, 2592.
(3) Smiglak, M.; Metlen, A.; Rogers, R. D. *Acc. Chem. Res.* **2007**, *40*, 1182.
(4) Zhao, H.; Holladay, J. E.; Brown, H.; Zhang, Z. C. *Science* **2007**, *316*, 1597.
(5) Huddleston, J. G.; Rogers, R. D. *Chem. Commun.* **1998**, 1765.
(6) Parnham, E. R.; Morris, R. E. *Acc. Chem. Res.* **2007**, *40*, 1005.
(7) Guerrero-Sanchez, C.; Lara-Ceniceros, T.; Jimenez-Regalado, E.; Rasa, M.; Schubert, U. S. *Adv. Mater.* **2007**, *19*, 1740.
(8) Li, Z.; Gessner, A.; Richters, J. P.; Kalden, J.; Voss, T.; Kubel, C.; Taubert, A. *Adv. Mater.* **2008**, *20*, 1279.
(9) Kaper, H.; Endres, F.; Djerdj, I.; Antonietti, M.; Smarsly, B. M.; Maier, J.; Hu, Y. S. *Small* **2007**, *3*, 1753.
(10) Ding, K.; Miao, Z.; Liu, Z.; Zhang, Z.; Han, B.; An, G.; Miao, S.; Xie, Y. *J. Am. Chem. Soc.* **2007**, *129*, 6362.
(11) Antonietti, M.; Kuang, D.; Smarsly, B.; Zhou, Y. *Angew. Chem., Int. Ed.* **2004**, *43*, 4988.
(12) Zhang, C.; Chen, J.; Zhou, Y.; Li, D. *J. Phys. Chem. C* **2008**, *112*, 10083.
(13) Jacob, D. S.; Bitton, L.; Grinblat, J.; Felner, I.; Koltypin, Y.; Gedanken, A. *Chem. Mater.* **2006**, *18*, 3162.
(14) Bühler, G.; Thölmann, D.; Feldmann, C. *Adv. Mater.* **2007**, *19*, 2224.
(15) Liu, D. P.; Li, G. D.; Su, Y.; Chen, J. S. *Angew. Chem., Int. Ed.* **2006**, *45*, 7370.
(16) Buhler, G.; Feldmann, C. *Angew. Chem., Int. Ed.* **2006**, *45*, 4864.
(17) Endres, F. *ChemPhysChem* **2002**, *3*, 144.
(18) Wang, T.; Kaper, H.; Antonietti, M.; Smarsly, B. *Langmuir* **2007**, *23*, 1489.
(19) Green, M.; Rahman, P.; Smyth-Boyle, D. *Chem. Commun.* **2007**, 574.
(20) Mu, X.; Meng, J.; Li, Z.; Kou, Y. *J. Am. Chem. Soc.* **2005**, *127*, 9694.
(21) Zhou, Y.; Schattka, J. H.; Antonietti, M. *Nano Lett.* **2004**, *4*, 477.
(22) Pileni, M. P. *Nat. Mater.* **2003**, *2*, 145.
(23) Rodil1, E.; Aldous, L.; Hardacre, C.; Lagunas, M. C. *Nanotechnology* **2008**, *19*, 105603.
(24) Eastoe, J.; Gold, S.; Rogers, S. E.; Paul, A.; Tom Welton; Heenan, R. K.; Grillo, I. *J. Am. Chem. Soc.* **2005**, *127*, 7302.
(25) Hao, J.; Zemb, T. *Curr. Opin. Colloid Interface Sci.* **2007**, *12*, 129.
(26) Cheng, S.; Zhang, J.; Zhang, Z.; Han, B. *Chem. Commun.* **2007**, 2497.
(27) Gao, Y.; Zhang, J.; Xu, H.; Zhao, X.; Zheng, L.; Li, X.; Yu, L. *ChemPhysChem* **2006**, *7*, 1554.

Published on Web 07/10/2009

was also conducted to study the behavior of ILs in microemulsion systems.[28−30] As an example, the aggregation of some imidazolium-based ILs in aqueous solutions was observed, indicating the similarity to surfactants.[30−32] The polarity and solvation properties of ILs could be easily modified due to their diverse functional groups and structures, facilitating the formation of microemulsions with desired properties.

Rare earth (RE) ions bear unique electronic and optical characteristics arising from their 4f electrons. This made RE ions doped materials, such as $REPO_4$, REF_3, and RE_2O_3, find potential applications in phosphors, lasers, amplifiers, and biolabels.[33−44] As a result of the shield of the $5s^25p^6$ shell, RE luminescences arising from 4f intrashell transitions were sharp and photostable and had longer lifetimes. RE orthophosphates had been shown to be a useful host lattice for RE ions to produce phosphors emitting various colors. They were also known as heat-resistant and up-conversion materials. Various synthesis routes of $REPO_4$ nanocrystals, including the hydrothermal method,[38,44] sol−gel method,[45] microwave-assisted method,[16] and microemulsion method,[46] had been developed. However, ILs had not been used in the design of "oil-in-water" three-phase microemulsion systems to make inorganic nanocrystals. Meanwhile, improving the optical properties of these nanocrystals was always desirable.

Herein, a novel tributylphosphate/1-octyl-3-methylimidazolium halide/water (TBP/[Omim]Cl/H_2O) microemulsion system was used to synthesize RE phosphate nanocrystals, and uniform nanoparticles and one-dimensional nanowires of $REPO_4$, $REPO_4 \cdot xH_2O$ (RE = La, Ce, Pr, Nd, Sm, Eu, Gd, Tb), and RE ions doped $REPO_4 \cdot xH_2O$ were successfully made. Moreover, the surfaces of the as-prepared nanocrystals were capped with TBP, leading to the enhancement of their luminescence and facilitation of their dispersion in some imidazolium-based ILs.

To the best of our knowledge, this is the first "oil-in-water" microemulsion system with ILs as surfactant and without any cosurfactants for the formation of nanocrystals. This strategy is expected to be applicable for the synthesis of other RE salt nanocrystals, like vanadates and fluorides.

Experimental Section

Synthesis of 1-Methyl-3-octylimidazolium chloride ([Omim]Cl). The detailed synthetic and purification procedures were discussed elsewhere,[47,48] and the product was characterized using ^{1}H NMR, ^{13}C NMR, and IR (Supporting Information).

Synthesis of TBP Capped $REPO_4 \cdot xH_2O$ Nanocrystals. In a typical synthesis, 0.1 mmol RE nitrate is dissolved in 0.3 mL of tributylphosphate (TBP), and then 10 mL of solution containing 0.005 mol of [Omim]Cl was added to give a transparent microemulsion. A total of 1 mL of NaH_2PO_4 solution (0.1 M) was then added dropwise under ultrasonic conditions. The mixture was then transferred into a 15 mL Teflon lined stainless-steel autoclave and sealed. The autoclave was heated at 100 °C for 48 h and cooled naturally to room temperature. Finally, the nanocrystals were collected by centrifugation, washed with distilled water and alcohol several times, and dried in air at 70 °C for 24 h.

Synthesis of Uncapped Nanowires. Uncapped nanowires were obtained using the reference method,[44] and the hydrothermal temperature was 100 °C.

Instrumentation. ^{1}H and ^{13}C NMR spectra were collected on a Bruker Advance DRX400 spectrometer. Fourier transform infrared (FT-IR) spectra were collected at room temperature with a Bruker IFS 66 V instrument. The morphology and size of the as-synthesized products were observed under a scanning electron microscope (Hitachi S-4800) and a transmission electron microscope (JEM-3010). The structure and phase purity of the as-synthesized samples were determined using X-ray diffraction (XRD) analysis on a Bruker AXS D8 Advance Powder X-ray diffractometer (using Cu Kα radiation: $\lambda = 1.5418$ Å). The PL excitation and emission spectra were collected at room temperature on a Hitachi F-4500 spectrophotometer equipped with a 150 W xenon lamp as the excitation source. The luminescence decay curves were obtained from a Lecroy Wave Runner 6100 digital oscilloscope (1 GHz) using a tunable laser (pulse width = 4 ns, gate = 50 ns) as the excitation (Continuum Sunlite OPO).

Results and discussion

Both hexagonal and monoclinic phase of RE phosphates can be controllably synthesized when changing the reaction temperature. The hexagonal phase of $REPO_4 \cdot xH_2O$ (RE = La−Tb) nanocrystals was obtained at 100 °C. When the reaction temperature was raised to 150 °C, monoclinic $REPO_4$ nanocrystals were obtained. The XRD patterns shown in Figures 1 and 2 indicate that the $REPO_4 \cdot xH_2O$ (RE = La−Nd and Sm−Tb) nanocrystals were in pure hexagonal phase (their JCPDS numbers

(28) Moniruzzaman, M.; Kamiya, N.; Nakashima, K.; Goto, M. *ChemPhysChem* **2008**, *9*, 689.
(29) Patrascu, C.; Gauffre, F.; Nallet, F.; Bordes, R.; Oberdisse, J.; Lauth-Viguerie, N. d.; Mingotaud, C. *ChemPhysChem* **2006**, *7*, 99.
(30) Blesic, M.; Marques, M. H.; Plechkov, N. V.; Seddon, K. R.; Rebelo, L. s. P. N.; Lopes, A. n. *Green Chem.* **2007**, *9*, 481.
(31) Singh, T.; Kumar, A. *J. Phys. Chem. B* **2007**, *111*, 7843.
(32) Goodchild, I.; Collier, L.; Millar, S. L.; Prokes, I.; Lord, J. C. D.; Butts, C. P.; Bowers, J.; Webster, J. R. P.; Heenan, R. K. *J. Colloid Interface Sci.* **2007**, *307*, 455.
(33) Meiser, F.; Cortez, C.; Caruso, F. *Angew. Chem., Int. Ed.* **2004**, *43*, 5954.
(34) Kompe, K.; Borchert, H.; Storz, J.; Lobo, A.; Adam, S.; Moller, T.; Haase, M. *Angew. Chem., Int. Ed.* **2003**, *42*, 5513.
(35) Liu, J.; Li, Y. D. *Adv. Mater.* **2007**, *19*, 1118.
(36) Heer, S.; Lehmann, O.; Haase, M.; Gudel, H. U. *Angew. Chem., Int. Ed.* **2003**, *42*, 3179.
(37) Huo, Z.; Chen, C.; Chu, D.; Li, H.; Li, Y. *Chem.—Eur. J.* **2007**, *13*, 7708.
(38) Yan, R.; Sun, X.; Wang, X.; Peng, Q.; Li, Y. *Chem.—Eur. J.* **2005**, *11*, 2183.
(39) Stouwdam, J. W.; van Veggel, F. C. J. M. *Langmuir* **2004**, *20*, 11763.
(40) Lim, M. A.; Seok, S. I.; Chung, W. J.; Hong, S. I. *Opt. Lett.* **2008**, *31*, 201.
(41) Yan, Z. G.; Yan, C. H. *J. Mater. Chem.* **2008**, *18*, 5046.
(42) Li, Q.; Yam, V. W. W. *Angew. Chem., Int. Ed.* **2007**, *46*, 3486.
(43) Gacoin, A. L.; Boilot, T.; Pierre, J. *Acc. Chem. Res.* **2007**, *40*, 895.
(44) Fang, Y. P.; Xu, A. W.; Song, R. Q.; Zhang, H. X.; You, L. P.; Yu, J. C.; Liu, H. Q. *J. Am. Chem. Soc.* **2003**, *125*, 16025.
(45) Yu, M.; Lin, J.; Fu, J.; Zhang, H. J.; Han, Y. C. *J. Mater. Chem.* **2003**, *13*, 1413.
(46) Xing, Y.; Li, M.; Davis, S. A.; Mann, S. *J Phys. Chem. B* **2006**, *110*, 1111.
(47) Huddleston, J. G.; Visser, A. E.; Reichert, W. M.; Willauer, H. D.; Broker, G. A.; Rogers, R. D. *Green Chem.* **2001**, *3*, 156.
(48) Burrell, A. K.; Sesto, R. E. D.; Baker, S. N.; McCleskey, T. M.; Baker, G. A. *Green Chem.* **2007**, *9*, 449.

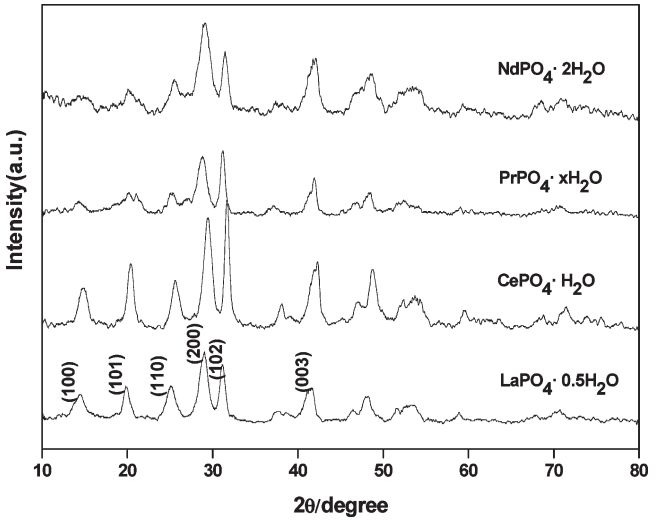

Figure 1. XRD patterns of $REPO_4 \cdot xH_2O$ nanocrystals (RE = La to Nd).

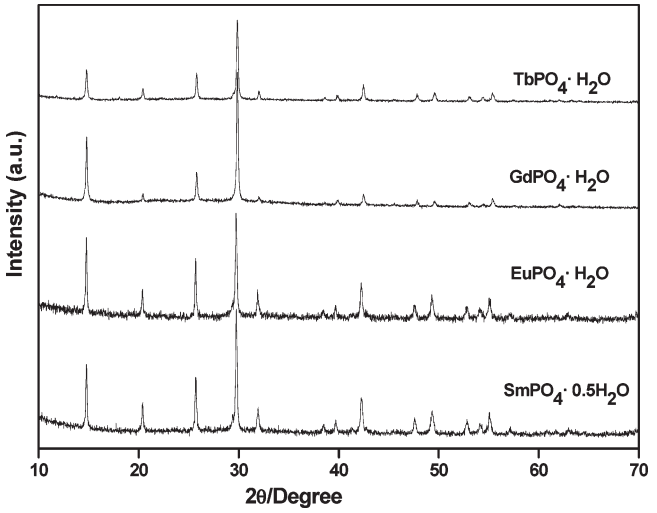

Figure 2. XRD patterns of $REPO_4 \cdot xH_2O$ nanocrystals (RE = Sm to Tb).

are 46-1439, 35-0614, 23-1202, 50-0620, 34-0537, 20-1044, 39-0232, and 20-1244, respectively). No peaks of any other phases or impurities were detected. Compared to light RE phosphates (RE = La−Nd), the XRD patterns of $REPO_4 \cdot xH_2O$ nanocrystals (Sm−Tb) exhibited sharp and narrow peaks, indicating their highly crystalline nature. Figure S1 (Supporting Information) showed the XRD patterns of monoclinic $LaPO_4$ and $CePO_4$ nanocrystals. All the reflections can be indexed to a pure monoclinic phase, and such a monoclinic structure was also identified for the other $REPO_4$ nanocrystals. These results indicated that the RE phosphate hydrate and RE phosphate nanocrystals were completely crystalline and in a pure phase.

The size and morphologies of the as-prepared structures were studied using SEM and TEM. Figure 3a shows the low magnification TEM images of the $CePO_4 \cdot H_2O$ nanowires. The HRTEM image (shown in Figure 3b) taken from a single nanowire showed the lattice spacing of 2.82 Å, which can be indexed to the (102) lattice space of $CePO_4 \cdot H_2O$. Under HRTEM (shown in Figure 3c), the $CePO_4 \cdot H_2O$ nanowires appear as a single crystal with

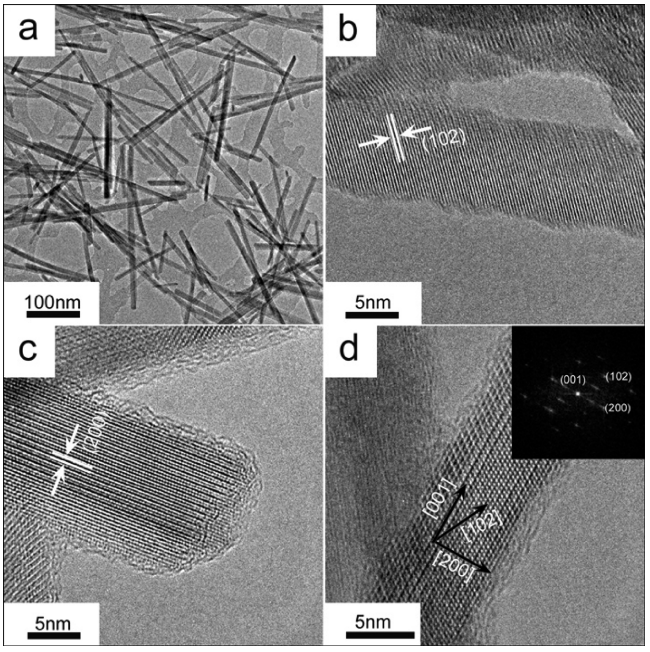

Figure 3. TEM and HRTEM images of $CePO_4 \cdot H_2O$ nanowires: (a) low magnification image and (b, c, d) HRTEM images of an individual nanowire.

a lattice spacing of 3.01 Å between two adjacent lattice planes parallel to the long axis, which was in good agreement with the theoretical *d*-spacing for (200) planes of hexagonal $CePO_4 \cdot H_2O$. The HRTEM image shown in Figure 3d displayed the clearly resolved planes of (200) and (102). The inset was the fast Fourier transform (FFT) analysis over the nanowire. The long axis of the nanowire was parallel to the {200} facets with an angle of 27.8° to the [102] direction, indicating the nanowires growing along the *c* axis. This is in very good agreement with the strong intensity of the (200) peak and (102) peak in the XRD patterns. According to the same hexagonal phase structures and synthetic conditions, it can be speculated that the other seven $REPO_4 \cdot xH_2O$ nanowires grew along the *c* axis.

Figure S2 (Supporting Information) showed the SEM images of hexagonal phase $LaPO_4 \cdot 0.5H_2O$, $CePO_4 \cdot H_2O$, $SmPO_4 \cdot 0.5H_2O$ $EuPO_4 \cdot H_2O$, $GdPO_4 \cdot H_2O$, and $TbPO_4 \cdot H_2O$, respectively. As shown in Figure S2a,b, the uniform $LaPO_4 \cdot 0.5H_2O$ and $CePO_4 \cdot H_2O$ nanowires were about 200−500 nm in length and their diameters were about 5−15 nm. From La to Nd, the RE phosphate hydrate nanowires had similar sizes and morphologies. But from Sm to Tb, the nanowires (shown in Figure S2c−f) had different sizes. Compared to the light RE phosphate hydrates (La to Nd), $SmPO_4 \cdot 0.5H_2O$ and $EuPO_4 \cdot H_2O$ nanowires (shown in Figure S2c,d) had similar diameters to those of $LaPO_4 \cdot 0.5H_2O$ nanowires but were much longer (up to 10 μm). $GdPO_4 \cdot H_2O$ and $TbPO_4 \cdot H_2O$ (shown in Figure S2e,f) nanowires were about 3−10 μm in length with diameters of 10−30 nm. The similar size difference among the RE phosphate hydrates prepared under same experimental conditions was also found in other reports.[38] Figure 4 showed an IR spectrum of the $CePO_4$ nanowires. Pure TBP had a ν(P═O) stretch at

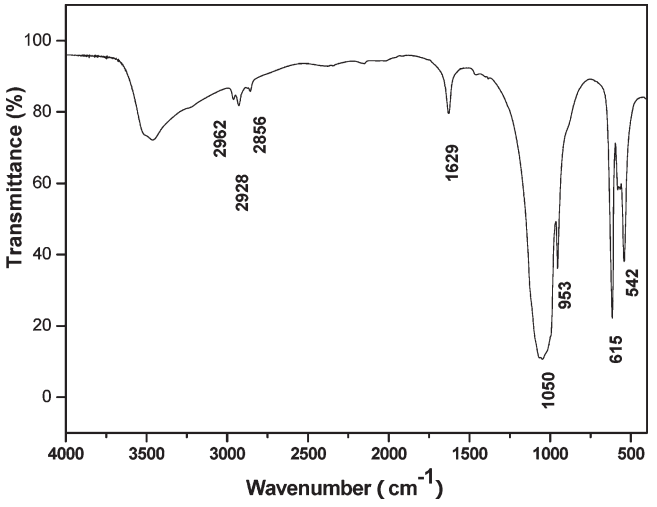

Figure 4. Fourier transform IR spectrum of $CePO_4 \cdot H_2O$ nanowires capped with TBP molecules.

1282 cm^{-1} and a ν(P−O−C) stretch between 950 and 1050 cm^{-1} but was heavily overlapped by the strong and broad peaks of PO_4^{3-} in our systems. But the peaks at 2928, 2856, and 2962 cm^{-1}, assigned to the antisymmetric and symmetric methylene stretches ($\nu_{as}(CH_2)$, $\nu_s(CH_2)$) and antisymmetric methyl stretches ($\nu_{as}(CH_3)$) of the TBP molecule, indicated the presence of the TBP molecules on the surfaces of the nanowires. The presence of TBP made the nanocrystals more easily dispersed in some imidazolium-based ILs, such as [Omim]Cl, [Omim]BF_4, [Omim]PF_6, and [Omim]Tf_2N.

Possible Mechanism. The surface, phase, and aggregation behaviors of ILs in solutions and mixtures with traditional solvents had attracted much research attention. Some molecular level based study had been brought forward in recent investigations. The aggregation behavior of 1-methyl-3-alkylimidazolium salts in aqueous solution had been studied.[30−32,49] The amphiphilic nature of IL cations can lead to nano-inhomogeneity. The critical micelle concentrations (CMC) and micelle structures of [Omim]Cl had been revealed by several groups.[30,32] It had been found that at concentrations just above the CMC, small near-spherical aggregates exist in aqueous [Omim]Br solutions, and the radius increases when increasing the concentration.[32] TBP was a well-known neutral organophosphorus extractant and had been extensively used in industrial extraction of RE ions for about half a century.[50] When extracting RE ions in a HNO_3 medium, $RE(NO_3)_3 \cdot 3TBP$ was formed as the extracted species.[50] Meanwhile, TBP was also a perfect solvent and capping agent in the synthesis of II−VI semiconductors.[51,52]

On the basis of the above results, a primary understanding of the nucleation and growth mechanism of the nanocrystals was proposed, as shown schematically in

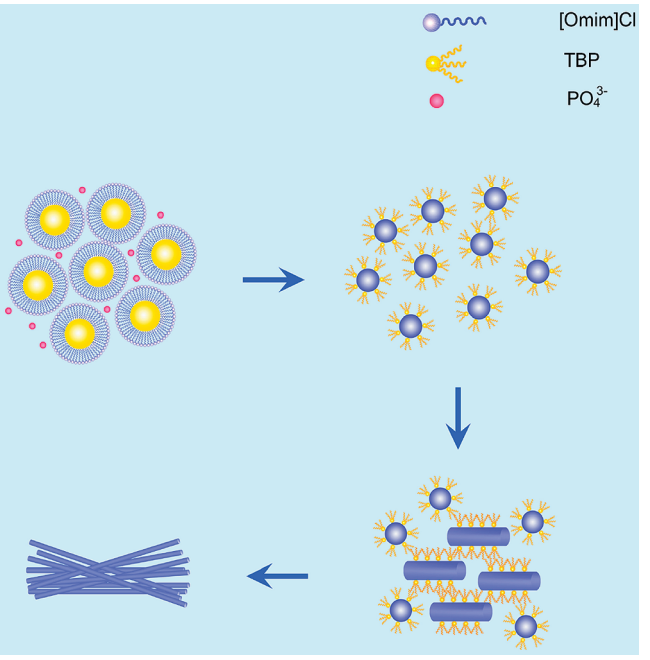

Figure 5. Schematic diagram showing the formation and growth processes of $REPO_4 \cdot xH_2O$ nanowires.

Figure 5. Both [Omim]Cl and TBP played key roles in the formation of the nanowires. On the basis of the proposed mechanism, when TBP containing RE ions were added to the mixture of water and [Omim]Cl, a micelle system was generated. TBP as the inner phase was confined by aggregated ILs with the hydrophobic carbon chains penetrating into the inner TBP phase and the imidazole rings pointing to the outer water phase. It was known that hydrophilic ILs existed in the form of ions in dilute aqueous solution instead of ion pairs. The coulomb interactions between PO_4^{3-} and imidazole rings make the ILs the buffer shell that suppresses the quick penetration of PO_4^{3-} into the micelles. After the injection of PO_4^{3-}, a homogeneous nucleation process would start in the micelles, thus producing uniform $REPO_4$ nanoparticles capped by TBP. In the following step, the nanoparticles with larger sizes would be able to grow into short nanorods at the expense of smaller ones through Ostwald ripening. It had been found the three carbon chains of TBP can facilitate the anisotropic growth of CdSe nanocrystals.[53] As a result of the different surface energies of different facets, the interaction between TBP and certain facets would be much stronger than others. Conjecturably, in the synthesis of $REPO_4 \cdot xH_2O$ nanowires, the newly formed side surfaces, {100} facets and {010} facets, might be stabilized by their interactions with the oxygen atoms of P═O groups in TBP. Meanwhile, the interaction between TBP and the two ends of the nanorods should be much weaker so as to enable the two ends of the nanorods to grow continuously through Ostwald ripening.[54,55] Thereby, after 48 h of reaction, uniform nanowires were generated as the products.

(49) Remsing, R. C.; Liu, Z.; Sergeyev, I.; Moyna, G. *J. Phys. Chem. B* **2008**, *112*, 7363.
(50) Marcus, Y. *Chem. Rev.* **1963**, *63*, 139.
(51) Peng, X.; Schlamp, M. C.; Kadavanich, A. V.; Alivisatos, A. P. *J. Am. Chem. Soc.* **1997**, *119*, 7019.
(52) Peng, Z. A.; Peng, X. *J. Am. Chem. Soc.* **2001**, *123*, 1389.
(53) Sapra, S.; Poppe, J.; Eychmuller, A. *Small* **2007**, *3*, 1886.
(54) Sun, Y.; Gates, B.; Mayers, B.; Xia, Y. *Nano Lett.* **2002**, *2*, 165.
(55) Sun, Y.; Mayers, B.; Herricks, T.; Xia, Y. *Nano Lett.* **2003**, *3*, 955.

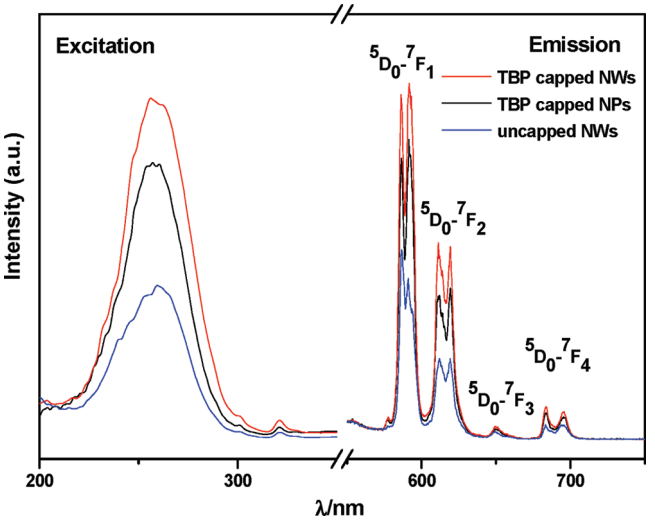

Figure 6. Emission spectrum (λ_{ex}: 254 nm) and excitation spectrum (λ_{em}: 591 nm) of $LaPO_4 \cdot 0.5H_2O$ nanocrystals doped with 10% Eu^{3+}: uncapped nanowires (blue), TBP capped nanoparticles (black), and nanowires (red).

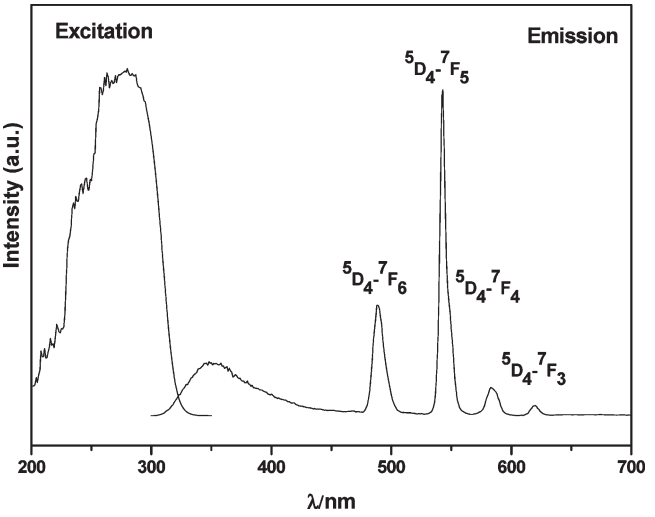

Figure 7. Emission spectrum (λ_{ex}: 285 nm) and excitation spectrum (λ_{em}: 542 nm) of $CePO_4 \cdot H_2O$ nanowires doped with 5% Tb^{3+}.

Figure S3a−c showed the morphologies of $LaPO_4 \cdot 0.5H_2O$ nanocrystals isolated from reactions with different times. As shown in Figure S3a, only nanoparticles were observed at the early ripening stage. When increasing the reaction time, short nanorods started to appear (shown in Figure S3b), and after a long ripening period of 48 h, they slowly grew into uniform nanowires along the *c* axis (shown in Figure S3c). It was also found that increasing the concentration of TBP sped up the growth process. The SEM observation of the nanocrystals at different stages was in good agreement with the conjecture.

Photoluminescence Properties. Figure 6 showed the excitation and emission spectra of hexagonal $LaPO_4$:Eu (10%) nanocrystals, including the uncapped nanoparticles and nanoparticles and nanowires capped with TBP. The broad charge-transfer band (CTB) centered at 254 nm, generating by electron delocalization from the filled 2p shell of O^{2-} to the partially filled 4f shell of Eu^{3+},[45] was in agreement with the previous reports on the bulk materials. The Eu^{3+} doped $LaPO_4$ nanocrystals exhibited orange-red luminescence (λ = 570−700 nm), assigned to transitions from the excited $^5D_0$ to the ^7F_J (J = 1−4) levels. It was well-known that the $^5D_0$-$^7F_1$ lines originate from magnetic dipole transition, while the $^5D_0$-$^7F_2$ lines originate from electric dipole transition. The electric dipole transition was allowed only on the condition that the europium ion occupied a site which was not an inversion center and was sensitive to local symmetry.[56] When Eu^{3+} ions occupied an inversion center, the $^5D_0$-$^7F_1$ transition should be relatively strong, while the $^5D_0$-$^7F_2$ transition should be relatively weak. In Figure 6, the intensity ratios of $^5D_0$-$^7F_2$ to $^5D_0$-$^7F_1$ in uncapped nanowires, TBP capped nanoparticles, and TBP capped nanowires were 0.61, 0.69, and 0.64, respectively. Compared to the nanoparticles, the TBP capped and uncapped nanowires had fewer surface atoms, and more Eu^{3+} occupied the site with inversion center and thus enhanced the $^5D_0$-$^7F_1$ transition.[57] Compared to the uncapped nanowires, the TBP capped nanoparticles and nanowires have higher emission intensity. Possible reasons might be that the capping TBP suppressed the quenching effect of the OH groups on the surfaces, and the influences from the effective index of refraction change.[39,56] The TBP capped nanowires had fewer surface defects than the nanoparticle, which contributed to the higher emission intensity. The luminescent decay curves of Eu^{3+} in $LaPO_4$ nanocrystals doped with 10% Eu^{3+} are shown in Figures S4−6 (Supporting Information). The $^5D_0$ lifetimes of Eu^{3+} in uncapped nanowires, TBP capped nanoparticles, and TBP capped nanowires were 2.85 ms, 3.70 ms, and 3.50 ms, respectively, indicating that the capping of TBP improved both the emission intensity and the lifetime of Eu^{3+} doped $LaPO_4$ nanocrystals.

The highly efficient energy transfer between Ce^{3+} and Tb^{3+} has made Ce^{3+} and Tb^{3+} coactivated $LaPO_4$ bulk powder a commercial green phosphor in fluorescent lamps, cathode ray tubes, and plasma display panels. Figure 7 gave the excitation and emission spectra of $CePO_4$ nanowires doped with 5% Tb^{3+}. The excitation spectrum was monitored by the $^5D_4$-$^7F_5$ emission. The broad excitation spectrum showed three peaks with maxima at 245, 263, and 280 nm, which corresponded to the transitions from the ground state of $^2F_{5/2}$ of Ce^{3+} to the different components of the excited Ce^{3+} 5d states split by the crystal field. Excitation in the Ce^{3+} absorption band at 285 nm yielded both the weak broad emission between 300 and 400 nm which arises from the 5d-4f emission of Ce^{3+} and the strong emission of Tb^{3+} (370−700 nm: $^5D_4$-^7F_J, J = 6, 5, 4, 3), showing the efficient energy transfer from Ce^{3+} to Tb^{3+}. In contrast to the f electrons of terbium, the d electrons of cerium strongly coupled to the lattice photons, resulting in broad overlapping bands and

(56) Liu, G.; Chen, X. Spectroscopic Properties of Lanthanides in Nanomaterials. Handbook on the Physics and Chemistry of Rare Earths; North Holland: Amsterdam, 2007; Vol. *37*, Chapter 233.

(57) Yu, L.; Song, H.; Lu, S.; Liu, Z.; Yang, L.; Kong, X. *J Phys. Chem. B* **2004**, *108*, 16697.

a significant Stokes shift. The luminescence decay curve of Tb^{3+} (Figure S7) in Tb^{3+} doped $CePO_4$ nanowires can be fitted to a single exponential function, and the lifetime of Tb^{3+} emission was 3.04 ms.

Conclusion

In summary, a novel ILs based "oil-in-water" microemulsion system was designed with [Omim]Cl as the surfactant. Uniform nanoparticles and one-dimensional RE phosphate nanowires were controllably obtained in this system. As a result of the capping of TBP on their surfaces, the as-prepared RE ion doped $REPO_4$ nanocystals had higher emission intensity and longer lifetimes than the uncapped ones. The surface modification by the TBP molecules facilitated their redispersion in some imidazolium-based ILs and extended their potential applications in IL-based luminescent soft materials. Moreover, this synthetic strategy was expected to be applicable for the synthesis of many other inorganic nanocrystals. This research should broaden the understanding of the behaviors and roles of ILs in the formation of inorganic nanocrystals and provided a facile strategy to prepare high quality inorganic nanocrystals.

Acknowledgment. This project was supported by National Natural Science Foundation of China (50574080) and the Distinguished Young Scholar Foundation of Jilin Province (20060114).

Supporting Information Available: XRD patterns of monoclinic $LaPO_4$ and $CePO_4$; SEM images of $REPO_4 \cdot xH_2O$ nanowires; SEM images of $LaPO_4 \cdot 0.5H_2O$ nanocrystals under different reaction times; decay curves of Eu^{3+} in $LaPO_4$:Eu^{3+} nanocrystals; decay curves of Tb^{3+} in $CePO_4$:Tb^{3+} nanowires; and ^1H NMR, ^{13}C NMR, and IR data of [Omim]Cl. This material is available free of charge via the Internet at http://pubs.acs.org.